ELSEVIER

A new method of ultrasound color flow mapping

Vera Behar [a,*], Dan Adam [a], Zvi Friedman [b]

[a] *Department of Biomedical Engineering, Technion-Israel Institute of Technology, Technion city, Haifa 32000, Israel*
[b] *GE Ultrasound Israel Ltd., Einstein Bldg, 7 Etgar St., Tirat Hacarmel 39120, Israel*

Abstract

Conventional ultrasound color flow mapping systems estimate and visualize only the axial velocity component. To obtain the transverse velocity component a modification of a multiple-beam method is proposed. The new two-dimensional color flow mapping system has a small size and consists of three transducers. The central transducer is an appodized and focused phased array. The other transducers are unfocused probes. Three transducers act as receivers and the central transducer operates as a transmitter. All receivers acquire rf scan lines that are then processed to estimate three axial velocity components using an autocorrelation method. These estimates are then combined to estimate the transverse velocity component, taking into account the geometric relationships among three transducers. Two algorithms for transverse velocity estimation are proposed. The first uses the Doppler angle estimate for calculation of the transverse velocity component. The other algorithm calculates the transverse velocity component directly from the axial components. The accuracy of the flow velocity estimators is estimated by simulations. Analysis of accuracy allows choosing the more effective algorithm for two-dimensional velocity estimation, which is insensitive to variations of the Doppler angle.
© 2003 Elsevier Science B.V. All rights reserved.

Keywords: Doppler processing; Autocorrelation; Ultrasound simulation

1. Introduction

In conventional commercial ultrasound systems, only the axial component of flow velocity can be estimated and visualized using the classic Doppler effect. The transverse component of flow velocity, however, is undetectable through the Doppler shift only. Therefore, in cases where a blood vessel is perpendicular to the axial dimension, no velocity estimate can be made. To extend flow velocity estimation to two- or three-dimensions, a number of techniques have been proposed [1–10]. The transverse flow velocity component can be found using the Doppler spectrum broadening effect (*spectrum bandwidth method*). In experimental studies, it is shown that the Doppler bandwidth is proportional to the velocity of scatterers crossing the ultrasound beam in the focus of a transducer [1–3]. A simple method for Doppler bandwidth estimation is described in [1]. It works well in conditions where the noise is below the threshold fixed at about 1% of the peak power. An effective algorithm for blood velocity estimation using the maximum Doppler frequency is presented in [2]. The received signal is analyzed through a computerized spectrum analyzer, which integrates all instantaneous spectra obtained over a selected interval of time. The maximum Doppler frequency is estimated from the ensemble-averaged spectrum, as the frequency where it crosses a fixed threshold. A simple method for constant flow velocity estimation that uses the classic and transverse Doppler effects is described in [3]. The main problem of this method is the real-time implementation for pulsated flow measurements because the Doppler angle and flow velocity must be estimated in a very short time to obtain accurate results. Instead of calculating the Doppler bandwidth based on a complete spectrum, the *correlation-based method* may be used to calculate variance of the spectrum. The transverse velocity is found using spectral variance as an approximation of the square of the Doppler bandwidth. This method is valid under the assumption that the transducer beamwidth is considerably smaller than the range cell length [4]. Another

---

* Corresponding author.
E-mail addresses: vera@biomed.technion.ac.il (V. Behar), dan@biomed.technion.ac.il (D. Adam), zvi.friedman@med.ge.com (Z. Friedman).

approach to find the transverse velocity vector is to use the *speckle tracking method* [5–7]. This method is based on the assumption that speckle translation closely reflects target translation at small displacements. The transverse velocity is measured by comparing the speckle patterns from consecutive laterally translated B-mode images. In the speckle tracking method described in [5], B-mode images are acquired by five parallel receive beams and one-dimensional correlations are calculated in order to estimate the three-dimensional velocity of blood flow. In each plane, one beam kernel in the center is tracked in both lateral directions. In particular, three beams in a plane are required whereas the method described in [6,7], however, requires only two parallel beams in a plane. The main problem of current speckle tracking methods is that the speckle patterns are more decorrelated at larger translations and a large number of computations are required for real-time implementation. The approach for two- or three-dimensional flow velocity estimation proposed by Fox is to use two or three transmit–receive beams crossing each other in region of interest (*multiple-beam method*) [8]. These beams may originate from discrete sub-apertures within the aperture of a single transducer [9] or from multiple transducers [8,10]. Two or more separate measurement coordinate systems are superimposed on the sample volume, and in each of which the axial velocity component is estimated. The estimates are then combined with geometrical relationships to obtain the two- or three-dimensional velocity vector. The real-time color mapping systems proposed exploit linear arrays with electronic scanning [9] or circular transducers with mechanical scanning [8,10]. To achieve adequate accuracy the angle separation between the transmit–receive beams needs to be sufficiently large. Therefore, a large transducer is required, if a single transducer is used for flow velocity estimation.

The technique presented in the paper extends the Fox approach described in [10] to conventional imaging in a sector. Unlike the Fox approach that requires two conventional transmit–receive probes for flow velocity estimation, the new color flow mapping system described here exploits three transducers. The central transducer operates as a transmitter, and all transducers act as receivers. The receivers acquire rf scan lines that are then processed to estimate three axial velocity components using an autocorrelation method. These estimates are then combined to estimate the transverse velocity component, taking into account the geometric relationships among three transducers. Two algorithms for transverse velocity estimation are proposed. The first uses the Doppler angle estimate for calculation of the transverse velocity component. The other algorithm calculates the transverse velocity component directly from the axial velocity components. The accuracy of the estimators is evaluated in simulations. Analysis of the

accuracy allows finding the more effective algorithm for flow velocity estimation that is insensitive to variations of the Doppler angle.

2. Axial velocity estimation

Consider a new imaging technique based on three transducers (Fig. 1). The central transducer is a focused phased array and the side transducers are unfocused probes. In transmit the narrow-angle beam of the central transducer is swept over the ROI in a polar sector scan, and a single transmit focus is set at the desired depth. In receive the central transducer (Receiver3) and two side transducers (Receiver1 and Receiver2) simultaneously receive the reflected and scattered field. In receive the dynamic focusing is applied only to the central transducer. Both transmit and receive apodization can be applied to the central transducer in order to reduce cross-correlation between signals acquired by receivers. The rf signals received are amplified, digitized, and recorded line by line until all scan lines are acquired. Because of the data acquisition, three sets of rf data are acquired by transducers and stored in the computer memory. To provide an axial velocity measurement the transmitter of an imaging system sends a pulse train along a single beam with a steering angle Θ. The pulse repetition time is T_{RP}. At each receiver (Receiver1, Receiver2 and Receiver3) the received signal is sampled at time $t = 2r/c$, where r is the distance to a desired sample volume (r_1—for Receiver1, r_2—for Receiver2 and r_3—for Receiver3). The samples of both quadrature components (in-phase and quadrature) of rf signals are obtained by a Hilbert transform. The complex signal formed by quadrature components is then used for estimation of the Doppler frequency shift. The Doppler frequency shift measured by Receiver1, Receiver2 and Receiver3 is Δf_1, Δf_2 and Δf_3, respectively. The Doppler frequency shift consists of two components. In order to find these components we consider a single scatterer T
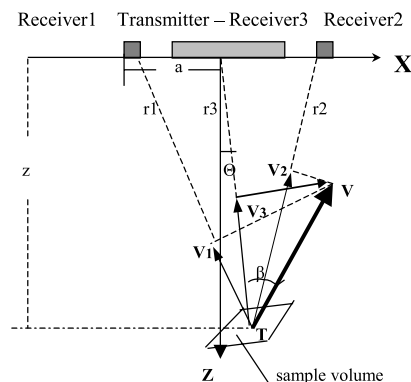

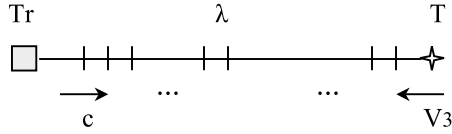Fig. 1. New method of two-dimensional velocity estimation.
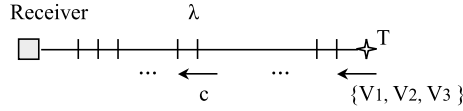
Fig. 2. Scatterer T moves towards the transmitter.

Fig. 3. Scatterer T moves towards the receiver.

traveling at linear velocity $\mathbf{V}$. In transmit mode a scatterer T travels towards the transmitter Tr at velocity V_3 as shown in Fig. 2. Therefore, the Doppler frequency shift indicated by a scatterer T is $f_{\text{shift,T}} = f_0 V_3/c$, where f_0 is the central frequency and c is the velocity of sound. In receive mode a scatterer T moves towards Receiver1 at velocity V_1, towards Receiver2—at velocity V_2 and towards Receiver3—at velocity V_3 as shown in Fig. 3. The Doppler frequency shift indicated by Receiver1, Receiver2 and Receiver3 is

$$f_{\text{shift,rec\_1}} = f_0 \frac{V_1}{c - V_1}; \quad f_{\text{shift,rec\_2}} = f_0 \frac{V_2}{c - V_2};$$
$$f_{\text{shift,rec\_3}} = f_0 \frac{V_3}{c - V_3} \tag{1}$$

The net Doppler frequency shift measured at Receiver1, Receiver2 and Receiver3 is

$$\Delta f_1 = f_0 \left(\frac{V_3}{c} + \frac{V_1}{c - V_1} \right); \quad \Delta f_2 = f_0 \left(\frac{V_3}{c} + \frac{V_2}{c - V_2} \right);$$
$$\Delta f_3 = f_0 \left(\frac{V_3}{c} + \frac{V_3}{c - V_3} \right) \tag{2}$$

Assuming that $V_1 \ll c$, $V_2 \ll c$ and $V_3 \ll c$, the expressions (2) take the form:

$$\Delta f_1 = f_0 \frac{V_3 + V_1}{c}; \quad \Delta f_2 = f_0 \frac{V_3 + V_2}{c}; \quad \Delta f_3 = 2 f_0 \frac{V_3}{c} \tag{3}$$

The axial velocity components V_1, V_2 and V_3 can be derived from Eqs. (3):

$$V_1 = \frac{c}{f_0} (\Delta f_1 - 0.5 \Delta f_3); \quad V_2 = \frac{c}{f_0} (\Delta f_2 - 0.5 \Delta f_3);$$
$$V_3 = \frac{c}{2 f_0} \Delta f_3 \tag{4}$$

The first order approximation of the mean shift frequency Δf_1, Δf_2 and Δf_3 is

$$\Delta f_1 = \frac{1}{2 \pi T_{\text{PR}}} \tan^{-1} \left[\frac{\text{Im} R_1(T_{\text{PR}})}{\text{Re} R_1(T_{\text{PR}})} \right];$$
$$\Delta f_2 = \frac{1}{2 \pi T_{\text{PR}}} \tan^{-1} \left[\frac{\text{Im} R_2(T_{\text{PR}})}{\text{Re} R_2(T_{\text{PR}})} \right];$$
$$\Delta f_3 = \frac{1}{2 \pi T_{\text{PR}}} \tan^{-1} \left[\frac{\text{Im} R_3(T_{\text{PR}})}{\text{Re} R_3(T_{\text{PR}})} \right] \tag{5}$$

where $R_1(\tau)$, $R_2(\tau)$ and $R_3(\tau)$ are the complex autocorrelation functions of signals received at Receiver1, Receiver2 and Receiver3, respectively. The complex autocorrelation function can be estimated by

$$R(m T_{\text{PR}}) = \frac{1}{M - m} \sum_{i=0}^{M-m} r^*(i T_{\text{PR}}) r((i + m) T_{\text{PR}}) \tag{6}$$

where $r(m T_{\text{PR}})$ is the sampled complex signal and M is the number of emissions. Using the estimates (5) and (6), the axial velocities V_1, V_2 and V_3 in (4) can be found as follows:

$$V_1 = \frac{c}{4 \pi f_0 T_{\text{PR}}} \left[2 \tan^{-1} \left(\frac{\text{Im} R_1(T_{\text{PR}})}{\text{Re} R_1(T_{\text{PR}})} \right) \right.$$
$$\left. - \tan^{-1} \left(\frac{\text{Im} R_3(T_{\text{PR}})}{\text{Re} R_3(T_{\text{PR}})} \right) \right] \tag{7}$$

$$V_2 = \frac{c}{4 \pi f_0 T_{\text{PR}}} \left[2 \tan^{-1} \left(\frac{\text{Im} R_2(T_{\text{PR}})}{\text{Re} R_2(T_{\text{PR}})} \right) \right.$$
$$\left. - \tan^{-1} \left(\frac{\text{Im} R_3(T_{\text{PR}})}{\text{Re} R_3(T_{\text{PR}})} \right) \right] \tag{8}$$

$$V_3 = \frac{c}{4 \pi f_0 T_{\text{PR}}} \tan^{-1} \left(\frac{\text{Im} R_3(T_{\text{PR}})}{\text{Re} R_3(T_{\text{PR}})} \right) \tag{9}$$

The estimates of axial velocities V_1, V_2 and V_3 can be used for calculation of the transverse velocity component $V_{3,\text{tr}}$. The flow velocity $\mathbf{V}$ can be expressed through its axial and transverse components:

$$|V| = \sqrt{|V_3|^2 + |V_{3,tr}|^2} \tag{10}$$

where $V_{3,\text{tr}}$ can be calculated by combining estimates V_1, V_2 and V_3 as shown below in the next section.

3. Transverse velocity estimation

The transverse velocity component $V_{3,\text{tr}}$ can be found combining the axial velocities V_1, V_2 and V_3 taking into account the geometric relationships among Receiver1, Receiver2 and Receiver3. The following two algorithms can be used for calculation of $V_{3,\text{tr}}$.

Algorithm 1. The transverse velocity component $V_{3,tr}$ can be found through estimation of the Doppler angle β (Fig. 1):
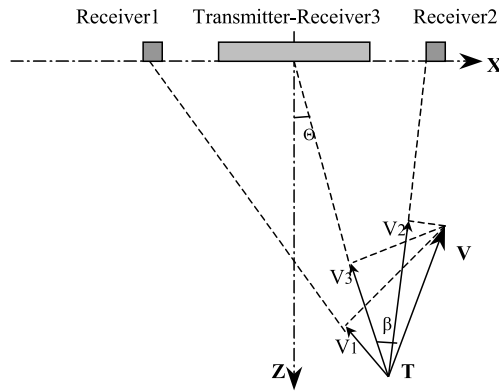
Fig. 4. Velocity **V** and its axial components (Case 1).

$$|V_{3,tr}| = |V_3| \tan(\beta), \quad 0 \leqslant \beta \geqslant \pi/2 \tag{11}$$

The Doppler angle β can be calculated using estimates of the axial velocity components V_1 and V_2. Consider the following four cases.

Case 1: The scatterer T is moving towards the Receiver1 and Receiver2, that is $V_1 > 0$ and $V_2 > 0$. The velocity of movement towards Receiver2 is greater than the velocity of movement towards Receiver1, i.e. $|V_2| > |V_1|$ (Fig. 4). Denoting the angle between V_1 and V_3 as α_1 and the angle between V_2 and V_3 as α_2 the absolute values of axial velocity components V_1 and V_2 can be written as follows:

$$V_1 = V \cos(\beta + \alpha_1) = V(\cos \beta \cos \alpha_1 - \sin \beta \sin \alpha_1);$$
$$V_2 = V \cos(\beta - \alpha_2) = V(\cos \beta \cos \alpha_2 + \sin \beta \sin \alpha_2) \tag{12}$$

Taking into account that $V_2 \# 0$ for $0 < \beta \leqslant \pi/2$, the ratio of V_1 and V_2 in (12) gives

$$V_1/V_2 = (\cos \beta \cos \alpha_1 - \sin \beta \sin \alpha_1)$$
$$/(\cos \beta \cos \alpha_2 + \sin \beta \sin \alpha_2) \tag{13}$$

Solving Eq. (13) for $\tan(\beta)$ one obtains

$$\tan(\beta) = (V_2 \cos \alpha_1 - V_1 \cos \alpha_2)$$
$$/(V_2 \sin \alpha_1 + V_1 \sin \alpha_2), \quad \text{where } \beta \# \pi/2 \tag{14}$$

Case 2: The scatterer T is moving towards the Receiver1 and Receiver2, that is $V_1 > 0$ and $V_2 > 0$. The velocity of movement towards Receiver2 is less than the velocity of movement towards Receiver1, that is $|V_2| < |V_1|$ (Fig. 5). In that case, the absolute values of the axial velocity components V_1 and V_2 can be written as follows:

$$V_2 = V \cos(\beta + \alpha_2) = V(\cos \beta \cos \alpha_2 - \sin \beta \sin \alpha_2);$$
$$V_1 = V \cos(\beta - \alpha_1) = V(\cos \beta \cos \alpha_1 + \sin \beta \sin \alpha_1) \tag{15}$$

Taking into account that $V_1 \# 0$ for $0 < \beta \leqslant \pi/2$, the ratio of V_2 and V_1 in (15) gives
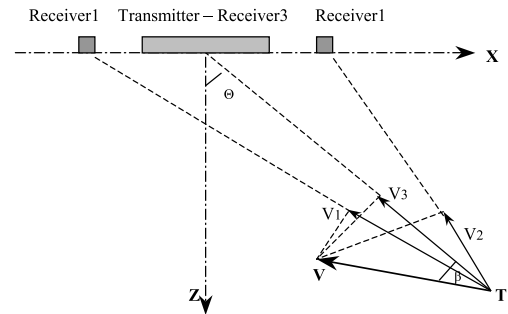

Fig. 5. Velocity **V** and its axial components (Case 2).

$$V_2/V_1 = (\cos \beta \cos \alpha_2 - \sin \beta \sin \alpha_2)$$
$$/(\cos \beta \cos \alpha_1 + \sin \beta \sin \alpha_1) \tag{16}$$

Solving Eq. (16) for $\tan(\beta)$, one obtains

$$\tan(\beta) = (V_1 \cos \alpha_2 - V_2 \cos \alpha_1)/(V_2 \sin \alpha_1 + V_1 \sin \alpha_2),$$
$$\text{where } \beta \# \pi/2 \tag{17}$$

Case 3: The scatterer T is moving towards Receiver2 and away Receiver1, that is $V_1 < 0$ and $V_2 > 0$. The velocity of movement towards Receiver2 is greater than the velocity of movement away Receiver1: $|V_2| > |V_1|$ (Fig. 6). In that case, the absolute values of the axial velocity components V_1 and V_2 can be written as follows:

$$V_2 = V \cos(\beta - \alpha_2) = V(\cos \beta \cos \alpha_2 + \sin \beta \sin \alpha_2);$$
$$V_1 = -V \cos(\beta + \alpha_1) = V(-\cos \beta \cos \alpha_1 + \sin \beta \sin \alpha_1) \tag{18}$$

Taking into account that $V_2 \# 0$ for $0 < \beta \leqslant \pi/2$, the ratio of V_1 and V_2 in (18) gives

$$V_1/V_2 = (-\cos \beta \cos \alpha_1 + \sin \beta \sin \alpha_1)$$
$$/(\cos \beta \cos \alpha_2 + \sin \beta \sin \alpha_2) \tag{19}$$

Solving Eq. (19) for $\tan(\beta)$, one obtains

$$\tan(\beta) = (V_1 \cos \alpha_2 + V_2 \cos \alpha_1)/(V_2 \sin \alpha_1 - V_1 \sin \alpha_2),$$
$$\text{where } \beta \# \pi/2 \tag{20}$$

Case 4: The scatterer T is moving towards Receiver1 and away Receiver2, that is $V_1 > 0$ and $V_2 < 0$. The velocity of movement away Receiver2 is less than the ve-
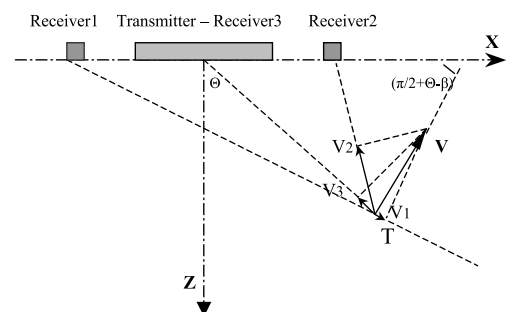

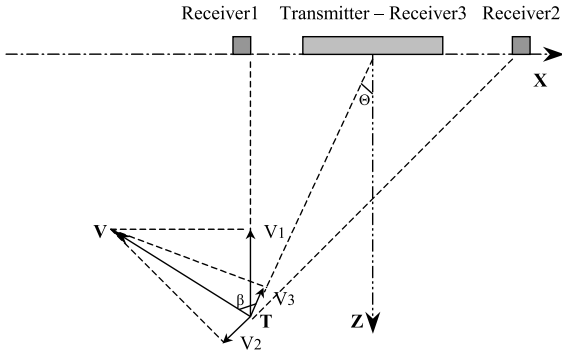Fig. 6. Velocity **V** and its axial components (Case 3).

Fig. 7. Velocity **V** and its axial components (Case 4).

locity of movement towards Receiver1, i.e. $|V_2| < |V_1|$ (Fig. 7).

In that case, the absolute values of the axial velocity components V_1 and V_2 can be written as follows:

$$V_2 = -V\cos(\beta + \alpha_2) = V(-\cos\beta\cos\alpha_2 + \sin\beta\sin\alpha_2);$$
$$V_1 = V\cos(\beta - \alpha_1) = V(\cos\beta\cos\alpha_1 + \sin\beta\sin\alpha_1) \tag{21}$$

Taking into account that $V_1 \# 0$ for $0 < \beta \leqslant \pi/2$, the ratio of V_2 and V_1 in (21) gives

$$V_2/V_1 = (-\cos\beta\cos\alpha_2 + \sin\beta\sin\alpha_2)$$
$$/(\cos\beta\cos\alpha_1 + \sin\beta\sin\alpha_1) \tag{22}$$

Solving Eq. (22) for $\tan(\beta)$, one obtains

$$\tan(\beta) = (V_1\cos\alpha_2 + V_2\cos\alpha_1)/(V_1\sin\alpha_2 - V_2\sin\alpha_1),$$
$$\text{where } \beta \# \pi/2 \tag{23}$$

Taking into account the expressions (11), (14), (17), (20) and (23), the final expression for calculation of the transverse velocity component $V_{3,\text{tr}}$ is

$$|V_{3,tr}| = |V_3| \cdot |(V_1\cos\alpha_2 - V_2\cos\alpha_1)/(V_1\sin\alpha_2 + V_2\sin\alpha_1)| \tag{24}$$

where $\sin\alpha_1$, $\sin\alpha_2$, $\cos\alpha_1$ and $\cos\alpha_2$ are computed for a fixed depth z using the following geometric relationships:

$$\sin\alpha_1 = a\cos\Theta \left/ \sqrt{a^2 + r_3^2 + 2ar_3\sin\Theta}\right.;$$
$$\sin\alpha_2 = a\cos\Theta \left/ \sqrt{a^2 + r_3^2 - 2ar_3\sin\Theta}\right.;$$
$$r_3 = z/\cos\Theta \tag{25}$$

and a is the distance between Receiver1 (or Receiver2) and Receiver3 (Fig. 1).

Algorithm 2. Another approach is to calculate $V_{3,\text{tr}}$ from estimates V_1, V_2 and V_3 without preliminary estimation of the Doppler angle. Consider the same cases mentioned above.

Case 1: Subtracting V_1 from V_2 in (12) and using that $V_{3,\text{tr}} = V\sin\beta$ and $V_3 = V\cos\beta$, we have:

$$V_{3,tr} = 0.5(V_3/\tan\alpha_1 - V_3/\tan\alpha_2 + V_2/\sin\alpha_2 - V_1/\sin\alpha_1) \tag{26}$$

Case 2: Subtracting V_1 from V_2 in (15) and using that $V_{3,\text{tr}} = V\sin\beta$ and $V_3 = V\cos\beta$, we have:

$$V_{3,tr} = 0.5(-V_3/\tan\alpha_1 + V_3/\tan\alpha_2 - V_2/\sin\alpha_2 + V_1/\sin\alpha_1) \tag{27}$$

Case 3: Summing V_1 and V_2 in (18) and using that $V_{3,\text{tr}} = V\sin\beta$ and $V_3 = V\cos\beta$, we have:

$$V_{3,tr} = 0.5(V_3/\tan\alpha_1 - V_3/\tan\alpha_2 + V_2/\sin\alpha_2 + V_1/\sin\alpha_1) \tag{28}$$

Case 4: Summing V_1 and V_2 in (21) and using that $V_{3,\text{tr}} = V\sin\beta$ and $V_3 = V\cos\beta$, we have:

$$V_{3,tr} = 0.5(-V_3/\tan\alpha_1 + V_3/\tan\alpha_2 + V_2/\sin\alpha_2 + V_1/\sin\alpha_1) \tag{29}$$

Taking into account directions of vectors V_1, V_2 and V_3, the expressions (26)–(29) can be merged, and the final expression for the calculation of the transverse velocity component $V_{3,\text{tr}}$ is

$$|V_{3,tr}| = 0.5|V_3/\tan\alpha_1 - V_3/\tan\alpha_2 + V_2/\sin\alpha_2 - V_1/\sin\alpha_1| \tag{30}$$

4. Implementation of velocity estimation

The axial velocity estimators (7)–(9) can be implemented as 2D- and 1D-techniques. The 2D technique relies on a two-dimensional autocorrelation approach to obtain estimates of V_1, V_2 and V_3. According to this approach, a window is selected by forming a complex data matrix of size $(N \times M)$, where N is the number of rf samples inside the window and M is the number of emissions. For each row of complex data, local estimates of both axial and transverse velocity are derived. Therefore, N local estimates of V_1, V_2, V_3 and $V_{3,\text{tr}}$ are obtained along the axial or depth axis of the window. The local estimates of $V_{3,\text{tr}}$ can be calculated using techniques Algorithm 1 or Algorithm 2 according to (24) or (30). The final estimates of both the axial and the transverse velocity components (V_3 and $V_{3,\text{tr}}$) are calculated by averaging of their N local estimates. The block diagram of the 2D-estimator of V_3 and $V_{3,\text{tr}}$ is presented in Fig. 8. The 1D-estimator uses only one value of a complex data per window along the depth axis, to obtain velocity estimates. This reduction in the signal dimensionality is achieved by integrating the complex data along the depth axis of the window before processing with the 1D autocorrelators. The axial velocity estimates V_1, V_2 and V_3 are obtained from the integrated data
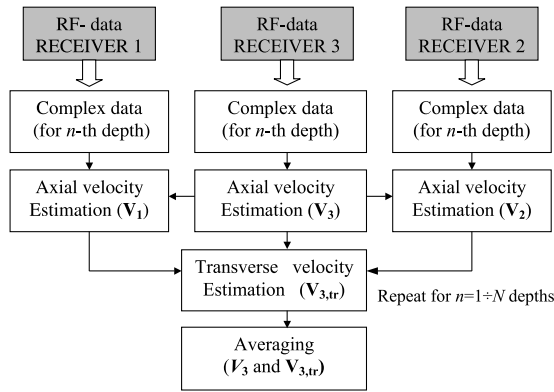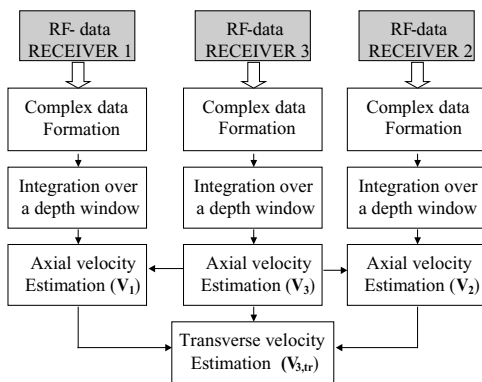
Fig. 8. Block diagram of the 1D-estimator.

Fig. 9. Block diagram of the 2D-estimator.

according to (7)–(9). The transverse velocity estimate $V_{3,tr}$ is calculated using the techniques Algorithm 1 or Algorithm 2 according to (24) and (30). The block diagram of the 1D-estimator of V_3 and $V_{3,tr}$ is presented in Fig. 9.

5. Simulation results and performance evaluation

The quality of velocity estimators is characterized in terms of their accuracy parameters that are the mean bias (Δ_V) and the standard deviation (σ_V) expressed as a percentage of the true velocity value:

$$\Delta_V = \frac{1}{VK} \sum_{k=1}^{K} \left| V - \widehat{V}_k \right| \times 100 \ [\%];$$

$$\sigma_V = \frac{1}{V} \sqrt{\frac{1}{K} \sum_{k=1}^{K} \left(\widehat{V}_k - E_V \right)^2} \times 100 \ [\%],$$

$$E_V = \frac{1}{K} \sum_{k=1}^{K} \widehat{V}_k \tag{31}$$

where E_V is the mean velocity estimate, $\widehat{V}_k$ is the current velocity estimate that is obtained in the kth simulation;

Table 1
System parameters used in the simulations, using Field II

Identification	Parameter	Value
Transmitter Receiver3	Number of elements	64
	Element width	0.29 mm
	Element height	13 mm
	Central frequency (f_0)	2.5 MHz
	Relative bandwidth (B)	62%
	Transmit focus	60 mm
	Excitation pulse length	3 cycles
	Apodization	Hanning
Receiver1 Receiver2	Distance "*Receiver_1 − Receiver_2*"	50 mm
Doppler processing	Repetition frequency (f_{PR})	5 kHz
	Sampling frequency	50 MHz
	Number of emissions (M)	16
	Size of a depth window (N)	16
	Maximal velocity (V_0)	0.5 m/s

K is the number of simulations and V is the true velocity value. The quality of velocity estimators is tested through simulations. The simulation is done using the program Field II [11]. Some of the relevant simulation parameters are given in Table 1. The simulated vessel has a diameter of 10 mm, and length of 80 mm. The center of the vessel is located 60 mm away from the central transducer surface. The angle between the vessel walls and the central transducer surface varies in the range [5–85°]. The vessel is simulated as a set of 6845 scatterers moving with a velocity, which is characterized by a parabolic distribution, $V(r) = V_0(1 - r^2/R^2)$, where r denotes the radial position of a point scatterer, R is the vessel radius, and V_0 is the maximal velocity at the center of the vessel. The positions of the scatterers are uniformly distributed inside the vessel. Their amplitudes have a random Gaussian distribution with a zero mean.

5.1. Velocity estimation in a sample volume

The simulation program generates for each emission ($i = 1, 2, \ldots, 16$) a file, which contains the positions and scattering strengths of point scatterers that correspond to the current emission time, and the corresponding rf scan line is thus simulated. The emission time is sampled at $1/f_{PR}$. Using the parameters of Table 1, 16 rf scan lines are simulated in order to calculate the current velocity estimate $\widehat{V}_k$. The number of repetitions (K) is 30. For the 2D-estimators, the current velocity estimate $\widehat{V}_k$ is calculated by averaging the local velocity estimates obtained at 16 points within a depth window located at a depth of 60 mm. The length of a depth window is chosen in accordance to the transmitted pulse length and is 1.8 mm. In the 1D-estimators, the current velocity estimate $\widehat{V}_k$ is formed after the rf signal integration within a depth window. The flow velocity to be estimated is 0.5 m/s. In order to quantify the influence of

flow direction on the accuracy of velocity estimation, all statistical measures (Δ_V, σ_V and E_V) are calculated for a large interval of the Doppler angle [5–85°]. In order to investigate how the accuracy of flow velocity estimation depends on the accuracy of estimation of axial and lateral components, the statistical measures (Δ_V, σ_V, E_V) are calculated for each velocity component (axial, lateral and flow), and for each estimation algorithm. Figs. 10 and 11 plot the statistical parameters (Δ_V, σ_V and E_V) of the axial velocity estimation, depending on the Doppler angle between the flow orientation and the central transducer surface. These parameters are obtained using the 2D- and 1D-estimators. It can be seen that the accuracy of the axial velocity estimation degrades with the increase of the Doppler angle. This effect is observed for both estimators. Indeed, both statistical parameters, the bias and the standard deviation do not exceed 10% as

long as the Doppler angle is less than 65°. The accuracy of the axial velocity estimation is drastically degraded when the Doppler angle exceeds 65°. However, according to (10), this drastic degradation of the axial velocity estimation does not cause drastic degradation of the flow velocity estimation because the values of the axial velocity become very small when the Doppler angle exceeds 75° and its influence on the flow velocity is small. In contrast to the axial velocity, the transverse velocity component increases with the increase of the Doppler angle as shown in Fig. 12. The corresponding accuracy parameters of the transverse velocity estimation are plotted in Figs. 13 and 14. The statistical measures of the flow velocity estimation are presented in Figs. 15–17. As shown in Figs. 12–14, the performance of both 2D- and 1D-estimators using the technique Algorithm 1 for transverse velocity estimation is drastically
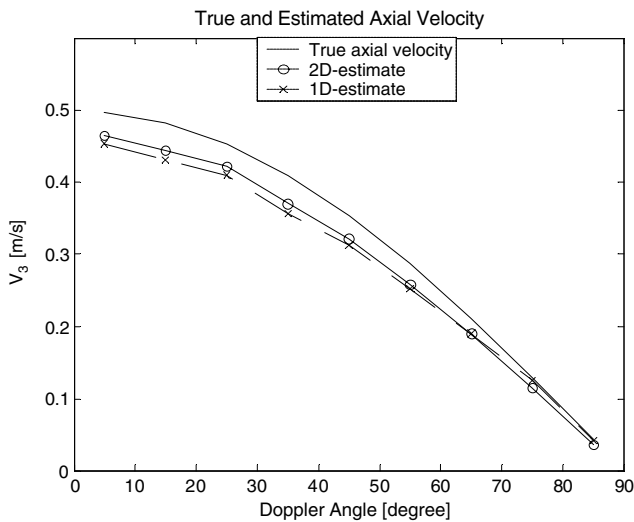

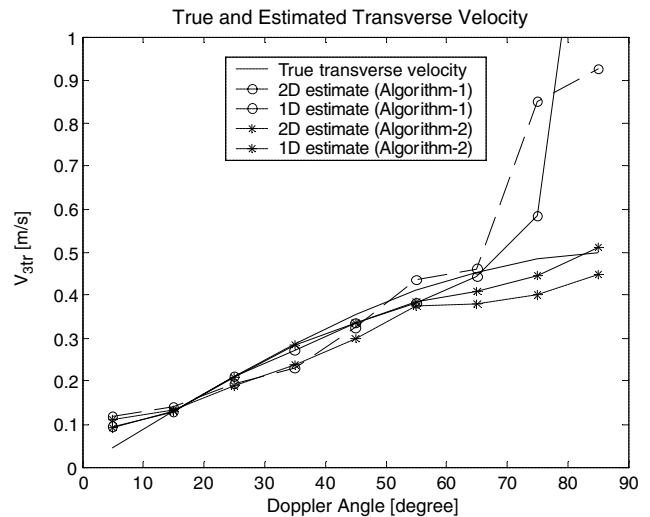Fig. 10. Mean estimate (E_V) of the axial velocity V_3.

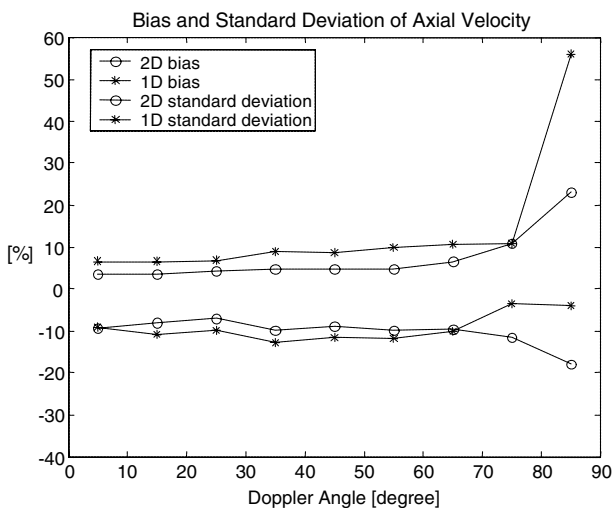Fig. 12. Mean estimate (E_V) of the transverse velocity $V_{3,tr}$.

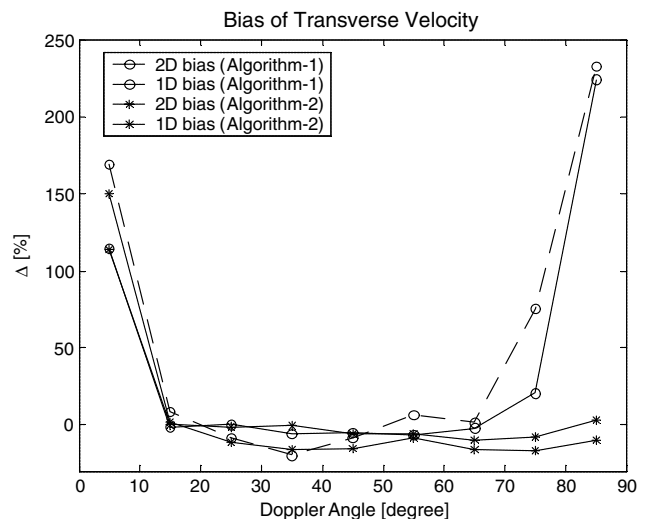Fig. 11. Accuracy (Δ_V, σ_V) of the axial velocity V_3.

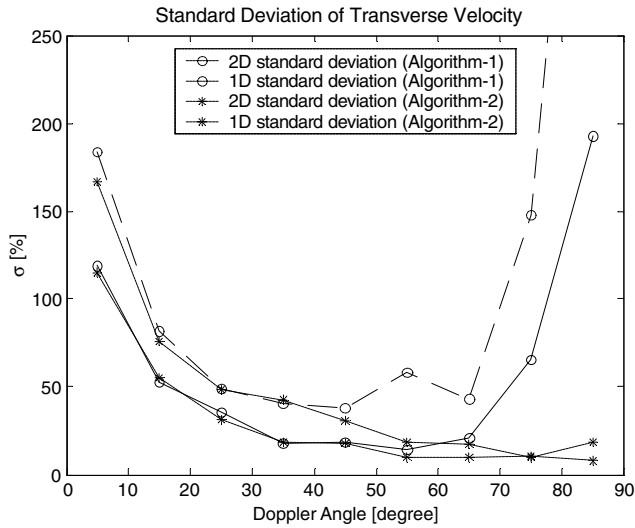Fig. 13. Bias (Δ_V) of the transverse velocity $V_{3,tr}$.

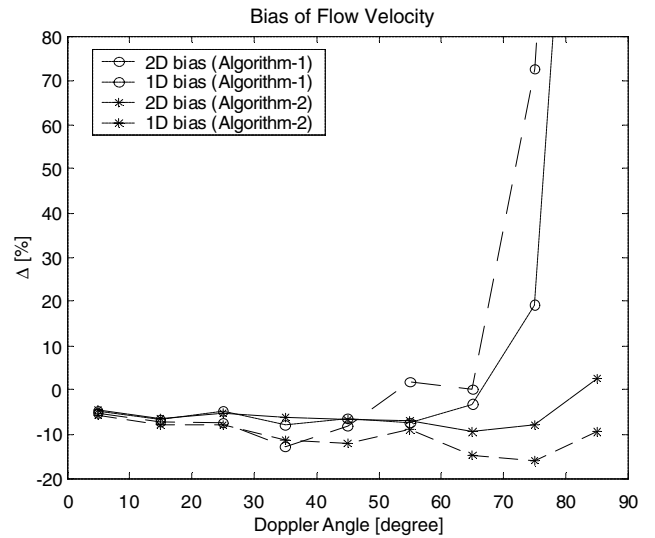Fig. 14. Standard deviation (σ_V) of the transverse velocity $V_{3,\text{tr}}$.

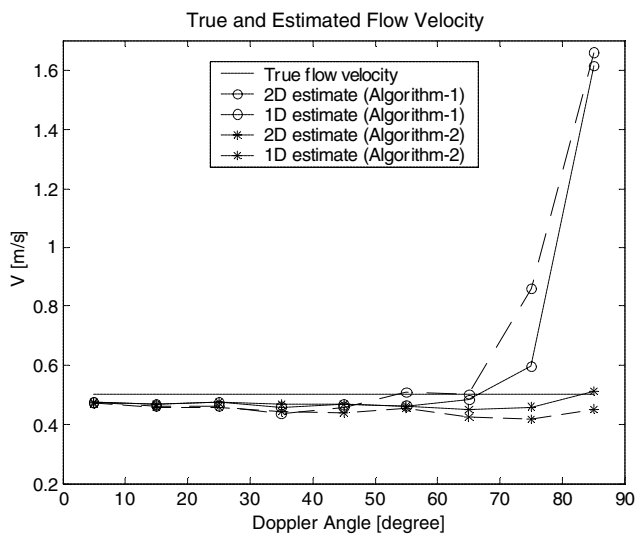Fig. 16. Bias (Δ_V) of the flow velocity **V**.

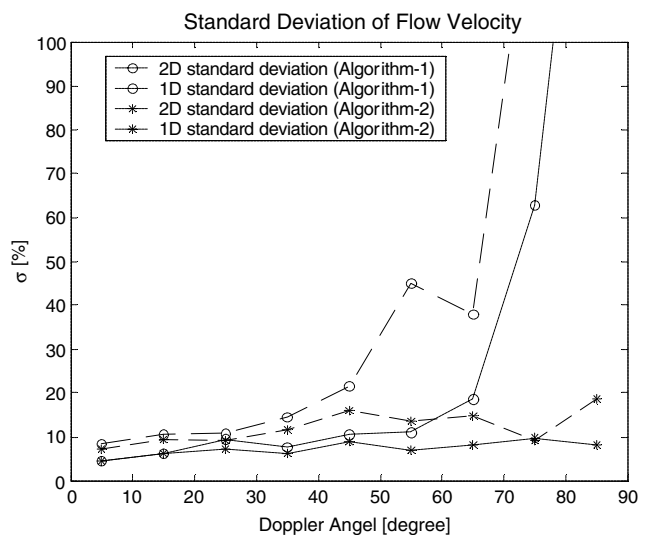Fig. 15. Mean estimate (E_V) of the flow velocity **V**.

Fig. 17. Standard deviation (σ_V) of the flow velocity **V**.

degraded when the Doppler angle exceeds 65°. This degradation occurs since the axial velocity components V_1 and V_2 used in (28) become very similar in value and opposite in sign. In contrast to the technique of Algorithm 1, the estimators employed by the technique of Algorithm 2 demonstrate accuracies that are independent of the Doppler angle. Indeed, both, the bias and the standard deviation vary in the range of 10% for the 2D-estimators and in the range of 15% for the 1D-estimators. As shown in Figs. 15–17, the accuracy of the transverse velocity estimation directly influences the flow velocity estimation. The estimators used in the technique of Algorithm 1 can be used only for the Doppler angles of less than 65°. On the other hand, the 2D-estimators used by the technique of Algorithm 2

demonstrate the best accuracy (<10%) in the entire range of the Doppler angle and is preferable for use in color flow mapping imaging.

5.2. Velocity profile estimation

A vessel with a laminar parabolic flow velocity profile is simulated using the program Field II. The maximal flow velocity (V_0) is 0.5 m/s. The angle between the ultrasound beam and the orientation of the vessel is 45°. A velocity profile is estimated along an axial line and consists of 16 points within the flow region. The entire axial line is divided into depth windows, each of 1.8 mm in length. The flow velocity estimation is done in each window. In order to study the effectiveness of the vari-

ous flow velocity estimators on the accuracy of flow velocity profile estimation, the statistical measures (Δ_V, σ_V, E_V) are calculated for four flow velocity estimators: (i) 2D-estimator using the technique of Algorithm 1; (ii) 1D-estimator using the technique of Algorithm 1; (iii) 2D-estimator using the technique of Algorithm 2; (iv) 1D-estimator using the technique of Algorithm 2. Figs. 18 and 19 depict the mean of the flow velocity profile estimates (E_V), obtained as the result of averaging of 30 profiles. The corresponding accuracy measures of the velocity profile estimation are shown in Figs. 20 and 21. It can be seen that all mean profiles are wider than the original profile and have bias of about 0.1 m/s within the vessel. A higher bias is observed near the walls of the vessel where the flow velocity is very small. The plots in Fig. 21 show that the real velocity profiles, however, are
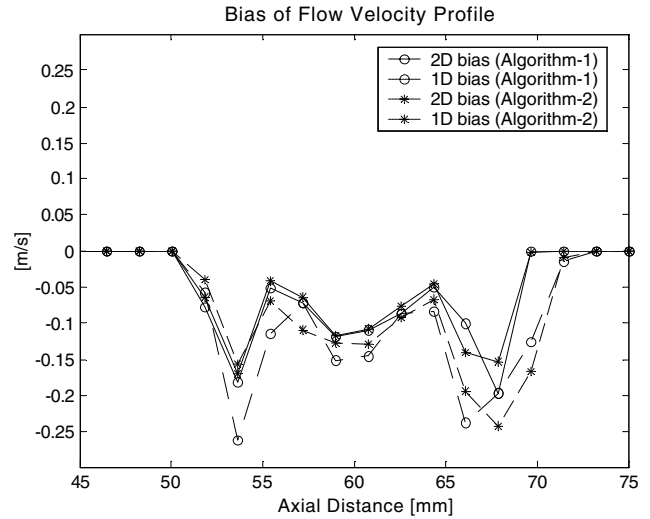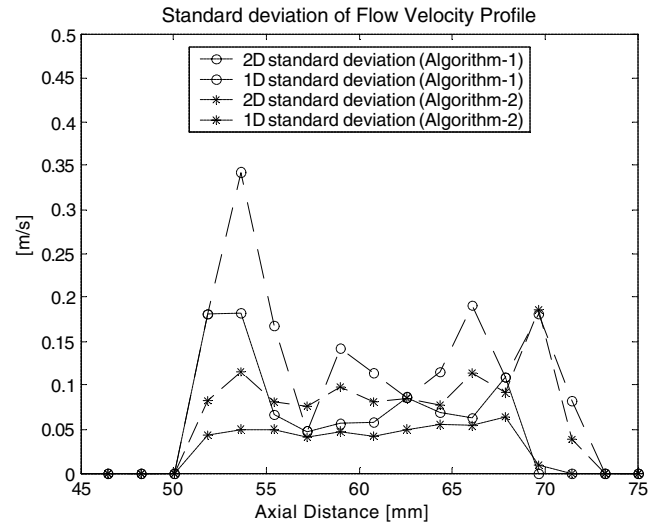

Fig. 20. Bias of the flow velocity profile [m/s].

Fig. 18. Estimated flow velocity profile (Algorithm 1).

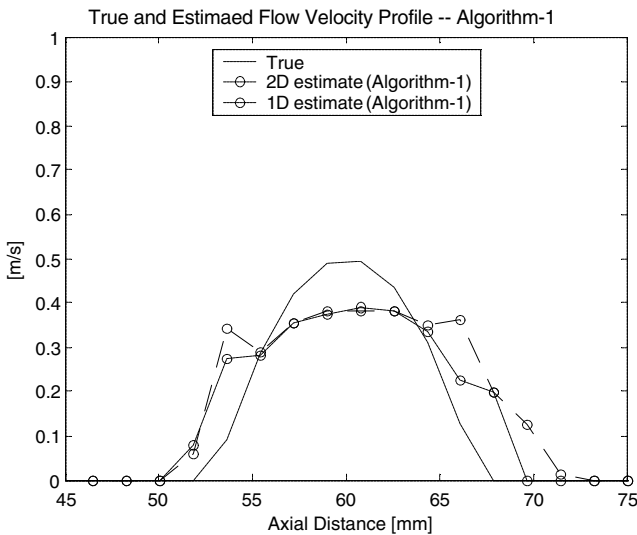

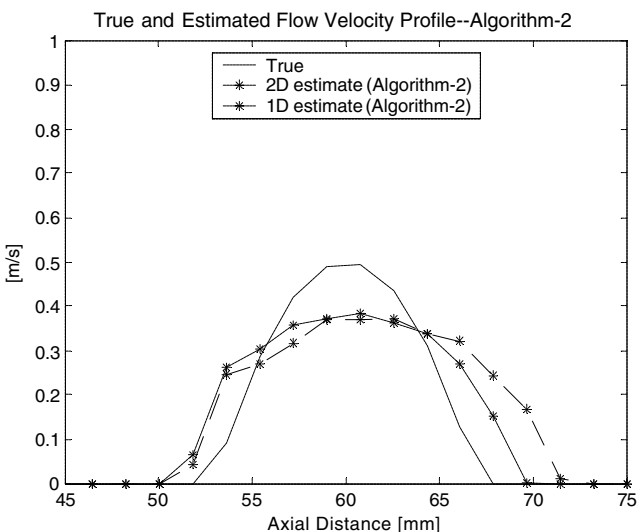Fig. 21. Standard deviation of the flow velocity profile [m/s].

within the ±3 standard deviations. Comparison analysis of the accuracy parameters of the flow velocity estimators shows that the 2D-estimator, using the technique of Algorithm 2 has the smallest bias and standard deviation along the entire axial line.

5.3. Color flow mapping

In order to demonstrate the capability of the flow velocity estimators to produce the color flow mapping (CFM) imaging four CFM-mode images are simulated. The flow phantom with a parabolic velocity profile is simulated using the program Field II. The simulation parameters are given in Table 1. In Figs. 22–25 the CFM-mode images are shown, as obtained for the four flow velocity estimators. It can be seen that all images

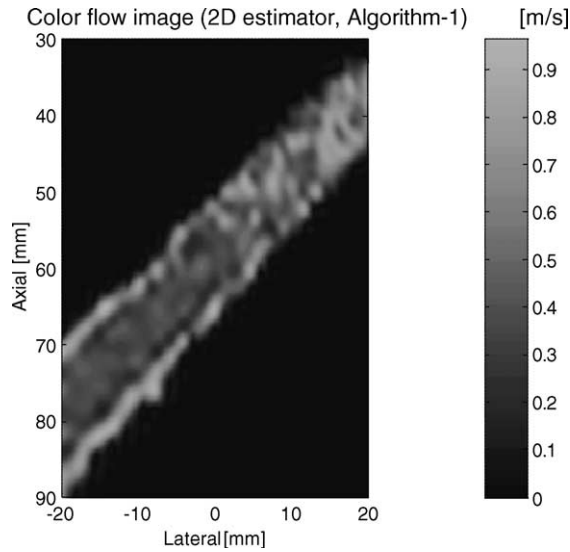Fig. 19. Estimated flow velocity profile (Algorithm 2).

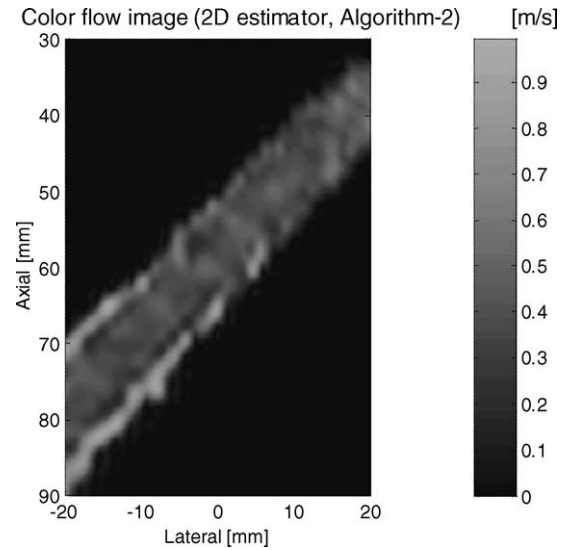Fig. 22. CFM-mode image (2D, Algorithm 1).

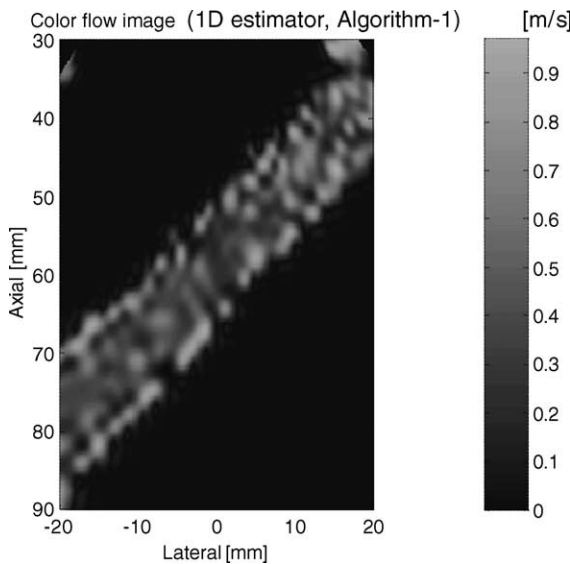Fig. 24. CFM-mode image (2D, Algorithm 2).
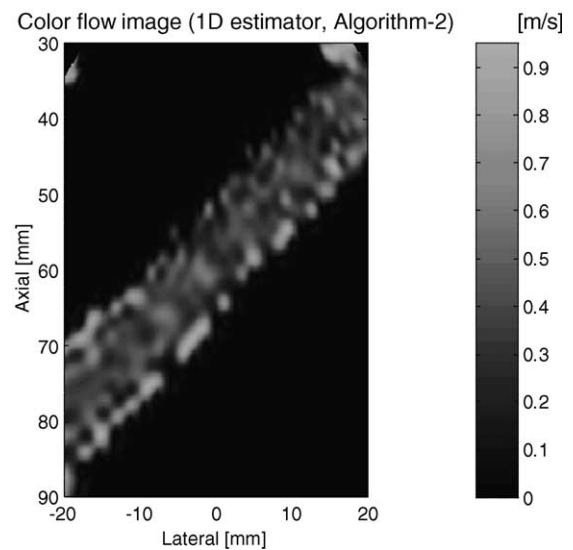

Fig. 23. CFM-mode image (1D, Algorithm 1).

Fig. 25. CFM-mode image (1D, Algorithm 2).

demonstrate the presence of artifacts near the walls of the flow phantom. However, the quality of the CFM-image obtained by the 2D-estimator using the technique of Algorithm 2 is the best, when compared to the other three images.

6. Conclusions

In this paper, we have presented a new method of flow velocity estimation using the multi-beam approach. The new method enables to produce flow velocity measurements and CFM images using the conventional imaging in a sector. In this method, three laterally separated

transducers (a phased array probe, and two pistons) estimate the axial components of the flow velocity in the same window in depth. The transverse velocity estimate is obtained as a combination of these axial velocity estimates. The new method demonstrates two advantages. Firstly, the transverse velocity estimate is achieved without decreasing the image frame rate because only a single transducer is used in the transmit mode. Secondly, the new method applies the multi-beam approach to CFM-imaging in a sector scan.

Two algorithms for transverse velocity estimation are proposed. The first uses the Doppler angle estimate to calculate the transverse velocity component. The other algorithm calculates the transverse velocity component

directly from the axial velocity estimates obtained by transducers.

Two techniques for implementation of the velocity estimation, 2D- and 1D-, are investigated by simulations. The accuracy of estimation is evaluated in terms of the accuracy parameters—the bias and standard deviation. Analysis of the simulation results shows that the 2D-estimator using the technique of Algorithm 2 is the most effective in terms of the accuracy parameters and is the least sensitive to variations of the Doppler angle.

Acknowledgements

References

[1] P. Tortoli, G. Guidi, C. Atzeni, A review of experimental transverse Doppler studies, IEEE Trans. Ultras. Ferro. Freq. Contr. 41 (1994) 84–89.

[2] P. Tortoli, G. Guidi, V. Newhouse, Improved blood velocity estimation using the maximum Doppler frequency, Ultrasound Med. Biol. 21 (1995) 527–532.

[3] B. Lee, H. Chiang, C. Kuo, W. Lin, S. Lee, Doppler angle and flow velocity estimations using the classic and transverse Doppler effects, IEEE Trans. Ultras. Ferro. Freq. Contr. 46 (1999) 252–256.

[4] P. Li, C. Cheng, C. Shen, Doppler angle estimation using correlation, IEEE Trans. Ultras. Ferro. Freq. Contr. 47 (2000) 188–196.

[5] O. Bonnefous, Measurement of the complete (3D) velocity vector of blood flows, IEEE Ultras. Symp. (1988) 795–799.

[6] L. Bohs, B. Geiman, M. Anderson, S. Breit, G. Trahey, Ensemble tracking for 2D vector velocity measurement: experimental and initial clinical results, IEEE Trans. Ultras. Ferro. Freq. Contr. 45 (1998) 912–924.

[7] L. Bohs, S. Gebhart, M. Anderson, 2-D motion estimation using two parallel receive beams, IEEE Trans. Ultras. Ferro. Freq. Contr. 48 (2001) 392–408.

[8] M.D. Fox, W. Cardiner, Three-dimensional Doppler velocimetry of flow jets, IEEE Trans. Biomed. Eng. 35 (1988) 834–841.

[9] P.J. Phillips, S.W. Straka, O.T. von Ramm, Real-time two-dimensional vector velocity color mapping ultrasound systems using sub-aperture pulse chasing, Ultras. Imag. 18 (1996) 60.

[10] M. Calzolai, L. Capineri, A. Fort, L. Masotti, S. Rocchi, M. Scabia, A 3-D PW Ultrasonic doppler flow-meter: theory and experimental characterization, IEEE Trans. Ultras. Ferro. Freq. Contr. 46 (1999) 108–113.

[11] J.A. Jensen, User's guide for the Field II program, Technical University of Denmark, 2001, August, [Online]. Available from <http://www.es.oersted.dtu.dk/staff/jaj/field/>.